Tectonophysics xxx (2009) xxx–xxx

Contents lists available at ScienceDirect

Tectonophysics

journal homepage: www.elsevier.com/locate/tecto

Destruction of Luzon forearc basin from subduction to Taiwan arc–continent collision

Justin Hirtzel [a], Wu-Cheng Chi [b,*], Donald Reed [a], Liwen Chen [b,c], Char-Shine Liu [c], Neil Lundberg [d]

[a] Department of Geology, San Jose State University, San Jose, CA 95192-0102, USA
[b] Institute of Earth Sciences, Academia Sinica, Taipei, Taiwan
[c] Institute of Oceanography, National Taiwan University, Taipei, Taiwan
[d] Department of Geology, Florida State University, Tallahassee, Florida, 08544, USA

ARTICLE INFO

Article history:
Received 3 July 2008
Received in revised form 17 January 2009
Accepted 29 January 2009
Available online xxxx

Keywords:
Arc
Forearc basin
Collision
Backthrust
Seismic profiles
Taiwan

ABSTRACT

Along offshore to the east of southern Taiwan, different stages of subduction and collision occur simultaneously along strike of the convergent boundary. As a result, the evolution of the Luzon arc and its forearc basin can be studied from the younger subduction zone to the south to the collision zone to the north. Examining more than 8000 km of seismic lines, we analyzed the seismic stratigraphy of strata in a forearc basin and its successive basins in the collision zone, to study the processes related to arc collapse and forearc basin closure. The study area presents three evolutional stages: intra-oceanic subduction, initial arc–continent collision, and arc–continent collision. We divided 9 seismic sequences in the forearc basin and found older, sub-parallel basin-fill sequences (4–9) and younger, divergent sequences (1–3). Isochron maps of the sequences were used to interpret different deformation modes and their areal extends. On the arc side of the basin of the subduction and initial collision zones, we found relatively undisturbed strata, showing little arc deformation. On the trench side, the growth strata in sequences 1 through 3 are the result of recent tectonic wedging along the rear of the accretionary prism. Tectonic wedging and back-thrusts incorporate the forearc strata into the rear of the accretionary prism until they close the forearc basin at a region with a 2200 m basement relief. This relief is not caused by active deformation, as young flat forearc strata lap onto it and mark the transition from initial collision to collision where many growth strata to the north suggest abrupt increase in active arc basement deformation. The (1) deforming basement, (2) back-thrusts, and (3) other sedimentary processes affect the architecture of the successive basins in the collision zone until the arc is juxtaposed to the rear of the fold and thrust belt on land.

1. Introduction

Arc–continent collision processes are important elements for continental growth (e.g. McCourt et al., 1984; Jahn, 2004; Jahn et al., 2004; Brown et al., 2001). However, it is still not clear if an arc and its forearc will be preserved as a whole during collision processes. If not, what part will be preserved and why? In other word, we want to study how the arc deforms and gets accreted or eroded during the collision? In addition, we want to know how the forearc basin strata response to the deformation of the arc and the rear of the accretionary prism, as the subduction progresses into an arc–continent collision. Here we used a detailed seismic stratigraphic analysis to study the deformation in the forearc basin and its basement to better understand the evolution of Luzon Arc and its forearc basin as they collide with the Chinese Passive Margin near Taiwan.

2. Tectonic setting

Here we will discuss the subduction, initial collision, and collision regions found around offshore Taiwan and also their northern extension in onland regions. We will then discuss the southward propagation of the collision process due to the oblique collision in the Taiwan region.

The offshore Luzon arc (Fig. 1) is along the boundary between the Eurasian plate and Philippine Sea plate where the oceanic lithosphere of the South China Sea is subducting eastward beneath the Philippine Sea plate (Bowin et al., 1978) with a rate of about 8 cm/yr (e.g. Yu et al., 1995), forming the Manila trench, Taiwan accretionary prism, North Luzon Trough (forearc basin), and Luzon arc.

Going north at about 20°50′N, subduction changes into an initial arc–continent collision where the continent–ocean boundary of the Chinese passive margin enters into the trench (Reed et al., 1992). Further to the north, the progressively thicker continental crust of the Eurasian plate enters into the convergent boundary. As a result, the wedge grows wider, incorporating basement materials into the wedge (Chi et al., 2003), and the width of the forearc basin starts to decrease until it is closed at about 21°20′N where the arc basement rises dramatically.

The closure of the North Luzon Trough marks the transition from initial collision to collision. Here, the Huatung Ridge is formed along the rear of the accretionary prism (Lundberg et al., 1997; Chen and Nakamura, 1998). This bathymetric high creates basin-filled sequences in the Southern Longitudinal Trough receiving detritus from

* Corresponding author. Fax: +886 2 27839871.
E-mail address: chi@earth.sinica.edu.tw (W.-C. Chi).

0040-1951/$ – see front matter © 2009 Elsevier B.V. All rights reserved.
doi:10.1016/j.tecto.2009.01.032

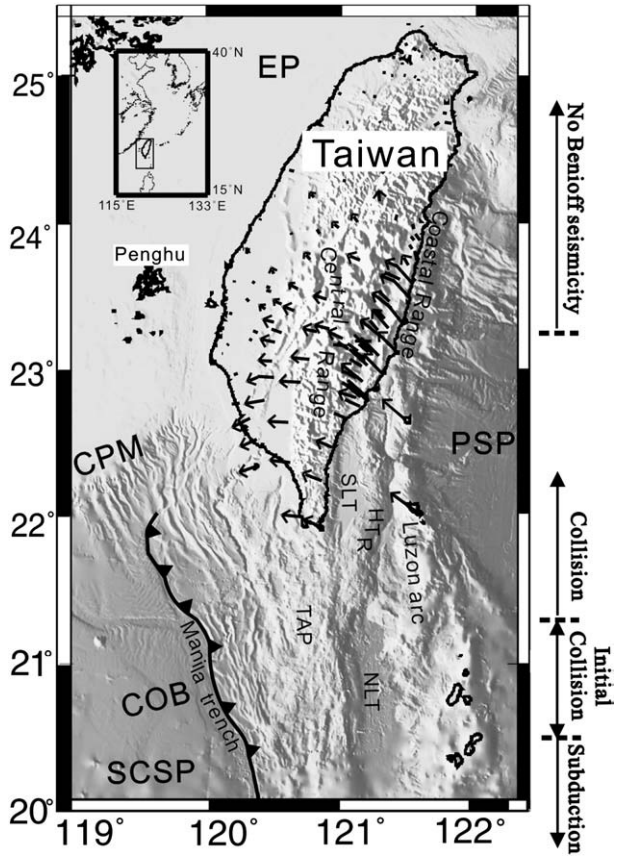

Fig. 1. Location map of Taiwan and regional tectonic setting. Here the oceanic South China Sea plate (SCSP) of the Eurasian plate (EP) is subducting southeastward at a rate of about 85 mm/year under the Philippine Sea plate (PSP) along the Manila trench forming the Taiwan accretionary prism (TAP), North Luzon Trough (NLT)—the forearc basin, and Luzon arc. The subduction changes into an initial arc–continent collision where the continent–ocean-boundary (COB) of the Chinese passive margin (CPM) enters into the trench. As a result, the accretionary prism grows larger. The initial collision changes into collision area where forearc basin is closed and the backthrusts form the Huatung Ridge (HTR), and its piggyback basin (the Southern Longitudinal Trough, SLT). Finally, the Luzon arc is juxtaposed next to the Central Range, a fold and thrust belt that is the northern extension of Taiwan accretionary prism. The Benioff seismicity associated with Luzon arc disappears abruptly north of 23°20′N. The arrows show the GPS relative motions with respect to the island of Penghu sitting on the stable Chinese continent.

southeastern Taiwan. During the collision process, the forearc basin and its basement are consumed until the Luzon volcanic arc is juxtaposed next to the fold and thrust belt of Taiwan onland in the mature collision zone (Lundberg et al., 1997; Cheng et al., 1998). By introducing shortening in the forearc basin basement in their sandbox models, Malavieille and Trullenque (2007) have successfully reproduced the shallow morphology and deformation in this region.

It is still not clear what happens to the consumed forearc basin basement. Several models have been proposed to explain the missing forearc basin basement. Based on compiled field studies, Teng (1990) proposes that part of the basement has been uplifted and exhumed as a response to the detachment of the slab. On the other hand, analog and numerical modeling suggests that a slice of forearc basement is subducted underneath the Luzon arc along an east-dipping lithospheric fault and can subduct a slice of forearc basement underneath the Luzon arc operating north of 21°30′N based on offshore seismicity data (Chemenda et al., 1997; Tang and Chemenda, 2000; Chemenda et al., 2001). This hypothesis is consistent with results from 2D traveltime inversions of both ocean bottom and onland seismic data (McIntosh et al., 2005) which have imaged a detached forearc block bounded by a steep east-dipping boundary fault illuminated by seismicity.

Further to the north onland, the Luzon arc extends into Coastal Range that consists of Miocene arc-related volcanic rocks unconformably overlain by sediments. To the west, the Taiwan fold and thrust belt, some of which is composed of continental units from the Chinese passive margin corresponds to the northern extension of the offshore Taiwan accretionary prism (Kim et al., 2005). As the Luzon arc approaches the Taiwan and Chinese passive margin, the volcanism ceases (Lo et al., 1994), but still exhibits remnant magmatic activities based on fission track dating and helium isotopic data of gas samples onland (Yang et al., 2003). The cessation of the volcanism is probably related to the over-thrust of the arc onto the passive margin on a major east-dipping listric fault as inferred from Carena et al. (2002). Based on paleomagnetic data, Lee et al. (1991) found a clockwise rotation, in map view, of the segmented Coastal Range as the arc rode onto the passive margin. However, the boundaries of each segment are still unknown. Lithological and field studies in the intra-arc regions onland found evidence of the arc which uplifted, subsided, and then again uplifted to its current position on land (Dorsey, 1992; Huang et al., 2006). There is no major forearc basin strata found onland. Convergent processes are still on-going, as slab earthquakes illuminate a clear east-dipping Benioff zone east of the Coastal Range. However, this seismic zone disappears abruptly north of 23.3°N.

Although the timing of initial collision is still under debate, Teng (1990) proposed that it probably began in the late middle Miocene and is currently propagating southward toward the modern subduction zone of offshore Taiwan at a rate of 55 to 120 mm/yr (Suppe, 1984; Lundberg et al., 1997; Byrne and Crepsi, 1997).

Due to the oblique collision in Taiwan region, different stages of the collision occurred simultaneously along the strike of the convergent boundary. The evolution of the arc and its forearc basin can be studied by constructing a series of cross sections, oriented east–west, through the subduction zone in the south to the more mature collision zone on Taiwan in the north (Suppe, 1984; Huang et al., 2006). Because of the oblique collision, the evolution of the Luzon arc can be studied not only by looking at the exposure on land, but also by analyzing offshore transects south of its current location. Similar concepts have been applied to study the evolution of the Taiwan accretionary prism (Chi et al., 2003; Chi and Dreger, 2004). Their results show progressive basement-involved deformation and exhumation in the accretionary prism from subduction to collision. Next we will use marine

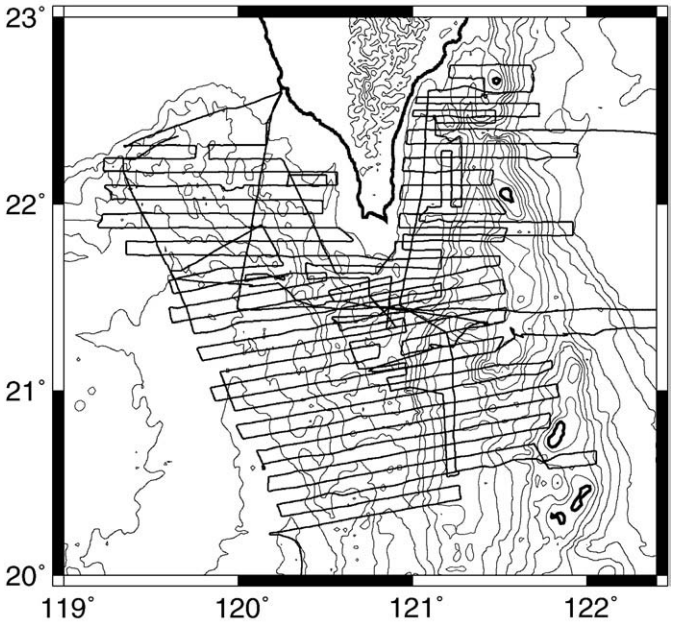

Fig. 2. Track chart of R/V *Moana Wave* cruise. We derive the seismic stratigraphy of the forearc basin using this dense dataset.

Please cite this article as: Hirtzel, J., et al., Destruction of Luzon forearc basin from subduction to Taiwan arc–continent collision, Tectonophysics (2009), doi:10.1016/j.tecto.2009.01.032

Table 1
Reflection data processing sequences

Moana Wave dataset
Resample to 4 ms
Geometry
Automatic gain control
Spiking deconvolution
Normal move out
Stack
Filter
Predictive deconvolution
Water-bottom mute
Trace weighting
Filter
Automatic gain control
4-fold stack section plot
F–K migration at 1500 m/s
Filter
Automatic gain control
Migrated section plot

geophysical data to study the evolution of the arc and its forearc basin from subduction to initial collision and collision.

3. Multi-channel seismic data acquisition, processing and results

We used a dense grid of 6 channel seismic profiles (Fig. 2) collected by the research ship R/V *Moana Wave* of the University of Hawaii (Reed et al., 1992; Liu et al., 1992; Lundberg, 1992) to study the forearc strata which covers an area of >50,000 km^2 from the Manila trench in the west to the Luzon island arc in the east by more than 8000 km of seismic lines. For this study, we focus on data east of the Taiwan accretionary prism. The seismic data were acquired using a 2-gun (460 in^3) array source and a 6-channel receiver with 25 m sections. A 37.5 m shot interval was used to produce a 4-fold CDP spaced at 25 m with an average line spacing of approximately 8 km. The data processing sequence is listed in Table 1. See Reed et al. (1992) for a more detailed description of the data processing.

In order to gain insight into the evolution of the North Luzon Trough and its successive basins to the north, we performed a seismic stratigraphic analysis of migrated seismic profiles and observations. Nine seismic sequences, with sequence 1 at the top, were recognized throughout the basin, especially in the subduction zone (Fig. 3, Table 2) wherein a detailed description of these strata can be found in Hirtzel (1996). We then discuss five seismic profiles representing different stages from the initial collision to collision (Fig. 4). Following that, the topography of the top of the arc basement is plotted and interpreted (Fig. 5). Finally isochron maps were generated for each sequence thickness (Fig. 6). In general, these maps show a south-westward increase in sediment thickness and depth to basement, which is clearly shown in a N–S seismic profile (Fig. 7) running parallel to the axis of the forearc basin.

In the subduction zone, the three dimensional shapes of the sequences range from layers to slightly wedge shaped deposits that lap onto the volcanic arc basement to the east. Basin-wide unconformities are not identified between these sequences in the central and eastern

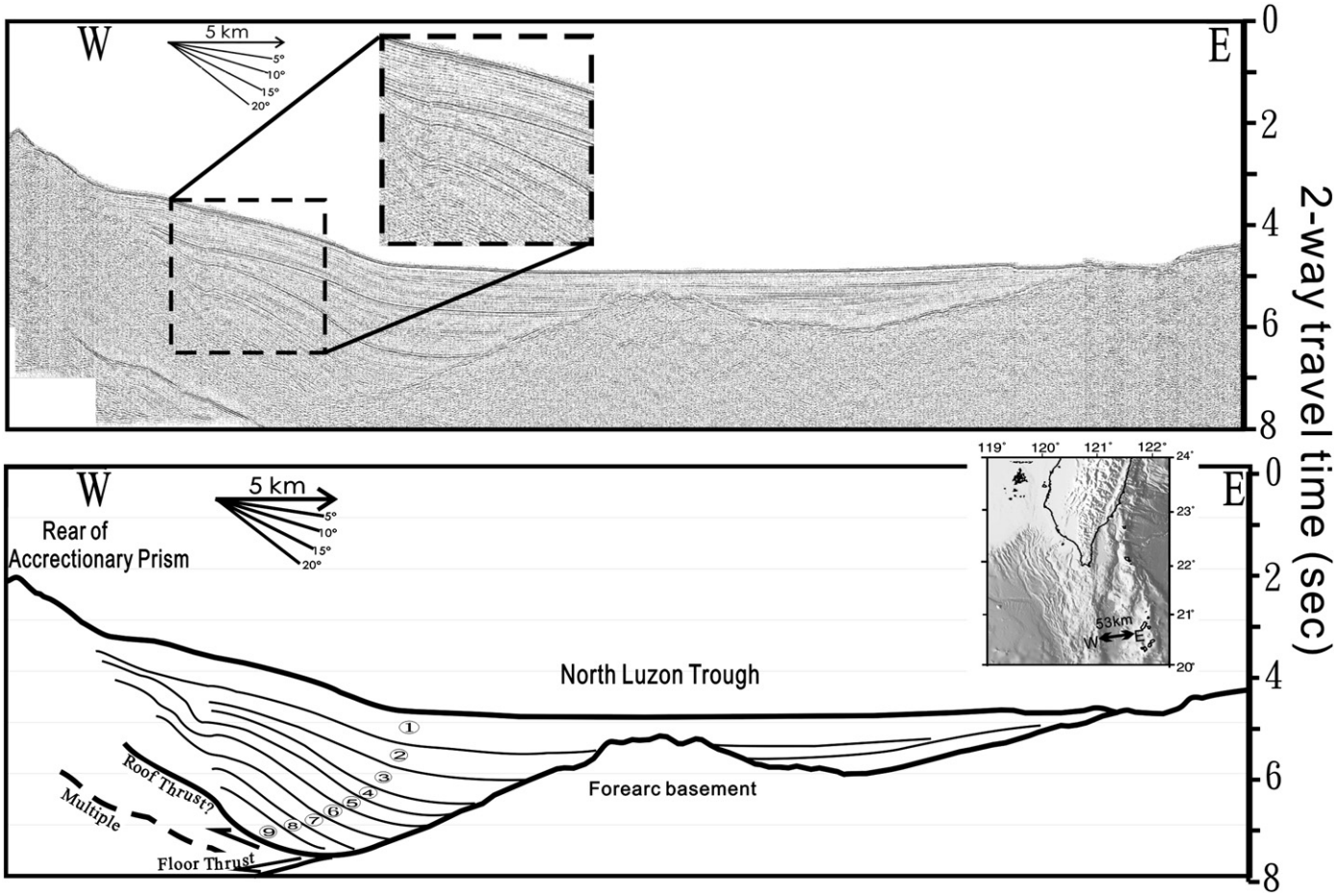

Fig. 3. A seismic profile in the subduction zone showing tectonic wedging and the nine seismic sequences derived from this study. Note the boundary between sequence 3 and sequence 4 marks the onset time of rapid uplift due to tectonic wedging. This line is unique in that a basement high under the forearc strata is clearly visible. We also found a possible unconformity on the eastern side of the forearc basin, which is not seen in other seismic profiles in the near-by region. Overall, we saw recent active uplift on the western side of the forearc basin but a relatively undeformed arc in the subduction.

Please cite this article as: Hirtzel, J., et al., Destruction of Luzon forearc basin from subduction to Taiwan arc–continent collision, Tectonophysics (2009), doi:10.1016/j.tecto.2009.01.032

Table 2
Description of the nine seismic sequences in the forearc basin (c.f. Fig. 6)

Sequence	Remarks
9	1. Oldest sequence imaged in the forearc basin. 2. Sequences 4 to 9 all show sub-parallel reflectors 3. Along the rear of the prism 4. Only found south of 21°10′N. 5. Shape like a three-dimensional wedge thinning to the north and west 6. West-ward thinning possibly related to early uplift along the rear of the prism
8	1. Similar characteristics to sequence 9 2. Extend a bit further north than sequence 9 3. Lesser degree of tilting in the west along the rear of the prism compared with sequence 9
7	1. Extending farther to the east. 2. Thinnest of the nine sequences 3. Wedge-shaped thinning to the north and west
6	1. Extending further east 2. Thinning between 20°55′N and 21°00′N
5	1. Similar to sequence 6, but covers a broader area 2. Wedge-shaped, thickening to the south
4	1. Thickening to the north and south
3	1. Marks a change in characteristics from the older sequences, which are composed mostly sub-parallel reflectors. 2. Reflectors are sub-parallel within the basin but converge to form a wedge-shaped body toward the rear of the prism. 3. Also present in successive basins to the north 4. Show localized chaotic reflectors characteristics of slump deposits
2	1. Similar to sequence 3
1	1. Youngest sequence 2. Blanket the forearc basin 3. Similar wedge-shaped geometry as sequences 2 and 3

regions of the basin. Reflectors also diverge to the east in the western region of the basin, are parallel within the center of the basin, and onlap the arc in the east (Fig. 3).

Further to the north in the initial collision zone, we found chaotic deposits on the western side of the forearc basin (Fig. 4e). The geometry of the arc basement becomes irregular (Fig. 4d). The arcward thrusts (back-thrusts) crop out to the seafloor and cause very complex faulting and folding patterns. The characteristics of reflectors within the center and arc side of the basin are similar to that in the subduction zone.

In the collision zone, the backthrusts extend to the north and form the Huatung Ridge, which grows arcward against a 60-km long basement high (Fig. 4, between 4d to 4b), and then again the arc (Fig. 4a). Growth strata overlies the northern end of this basement high (Fig. 4b). The internally deformed strata in the Southern Longitudinal Trough lap onto the Huatung Ridge. Growth strata and folded, eroded strata were observed in many places (Fig. 4) on both sides of the Huatung Ridge.

We then studied the topography of the arc basement from the subduction zone to the collision zone. Two-way traveltime from sea surface to the top of the basement was measured and plotted (Fig. 5). Overall, the basement deepens to the southwest, but there are also local depressions to the north. Because the plot is in two-way traveltime, some of the topographic relieves are affected by the geometries of the forearc strata and water body above the forearc basement. However, the first order features derived from this study should still be correct.

In addition, we have interpreted a N–S seismic line along the axis of the forearc basin (Fig. 7). The arc basement seems to be segmented into blocks each 40–60 km in length. There are minor disturbances in the overlying strata near the segmentation boundaries. In the intra-oceanic subduction zone, the arc basement is deeper than an 8 s two-way traveltime. However, the basement becomes shallower (~6 s) in the initial collision zone. To the north where the forearc basin is closed, we found relatively flat strata onlapping to the basement high. The arc basement becomes even shallower (~3 s) going from the initial collision zone to the collision zone to the north as seen from this profile and Fig. 4.

4. Interpretation of seismic stratigraphy

The seismic stratigraphic framework for the North Luzon Trough (the forearc basin) and its northern extension give us insight on how the forearc basin closes and the arc deforms. Notably, because the areal extend of the sequences decreases from sequence 1 to 9 the area we can only use stratigraphy data as passive markers for arc deformation is time dependant. Thus we are not able to study arc deformation further away from the depocenter for earlier and smaller sequences. On the other hand, we have wider spatial control for the younger sequences 1 through 3 that were possibly deposited during the collision period.

The lower sequences (4 through 9) can be grouped together due to the parallel relationship of their reflectors and sequence boundaries (Fig. 3). Sequences 8 and 9 represent the oldest deposited sediments that have not yet being fully incorporated into the tectonic wedge. Both sequences lap onto the rear of the accretionary prism and have been uplifted and tilted during the growth of the accretionary prism. The parallel relationship of reflectors and boundaries in sequences 4 through 7 suggest periods of relatively uniform sedimentation and little or no uplift from tectonic wedging. During this period, the depositional processes affecting forearc basin strata were dominated by broad sheet flows dispersing sediments widely throughout the basin.

In contrast to the parallel reflectors of sequences 4 through 7, the upper three sequences show a convergence of their boundaries to the west (Fig. 3). This observation, along with areas of chaotic reflectors characteristic of slump deposits, suggests that the area has recently experienced a period of uplift. Thus, the boundary between sequences 3 and 4 can be interpreted as the time of onset of uplift along the rear of the accretionary prism.

5. Discussion

Here, we will note the deformation modes in subduction zone, initial arc–continent collision zone, and arc–continent collision zone.

5.1. Intra-oceanic subduction (south of 20°50′N)

The inferred uplift while sequences 1 to 3 were deposited (Fig. 3) is probably caused by tectonic wedging first proposed by Reed et al. (1992) and studied in detailed by Chi et al. (2003). This process involves a wedge of accretionary prism material moving eastward beneath the basin sequences via a floor and roof thrust system. As a result, the tectonic wedge lifts the western edge of the forearc basin sequences 4 to 7 while sequences 1 to 3 were deposited. The floor and roof thrusts work together to bring western parts of sequences 4 to 9 into the tectonic wedge in the subduction zone. There is a possibility of even older sequences that used to be in the forearc basin now being incorporated into the tectonic wedge. The roof thrust is eventually cut at a shallower depth by backthrusting along east-vergent thrusts, resulting in the incorporation of forearc basin sediments into the rear

Fig. 4. Several seismic profiles showing the evolution of the Luzon arc and its forearc basin in the initial collision zone north of 20°50′N. As shown in Fig. 3 in the subduction zone, we found 9 seismic sequences, of which the top 3 sequences are tilted as a result of tectonic wedging under the rear of the accretionary prism. The backthrusts along with tectonic wedge tilt and incorporate the forearc strata into the rear of the forearc basin. Fig. 4e shows chaotic deposits with sediments from the rear of the accretionary prism and Huatung Ridge. Fig. 4d is located in the region where there is a 2200 m relief in arc basement forcing the backthrusts to crop out. Surficial processes are active as part of the folded strata gets eroded. We interpreted more out-of-sequence backthrusts and growth strata in Fig. 4c. In Fig. 4b, we saw a mature Huatung Ridge (HTR), and the growth strata in front of it. As collision progresses, the growth strata is incorporated into the Huatung Ridge. Then, in Fig. 4a we can see the piggyback basin (Southern Longitudinal trough) is formed with some internal deformation. Overall, we saw a variety of active deformations in this region.

Please cite this article as: Hirtzel, J., et al., Destruction of Luzon forearc basin from subduction to Taiwan arc–continent collision, Tectonophysics (2009), doi:10.1016/j.tecto.2009.01.032

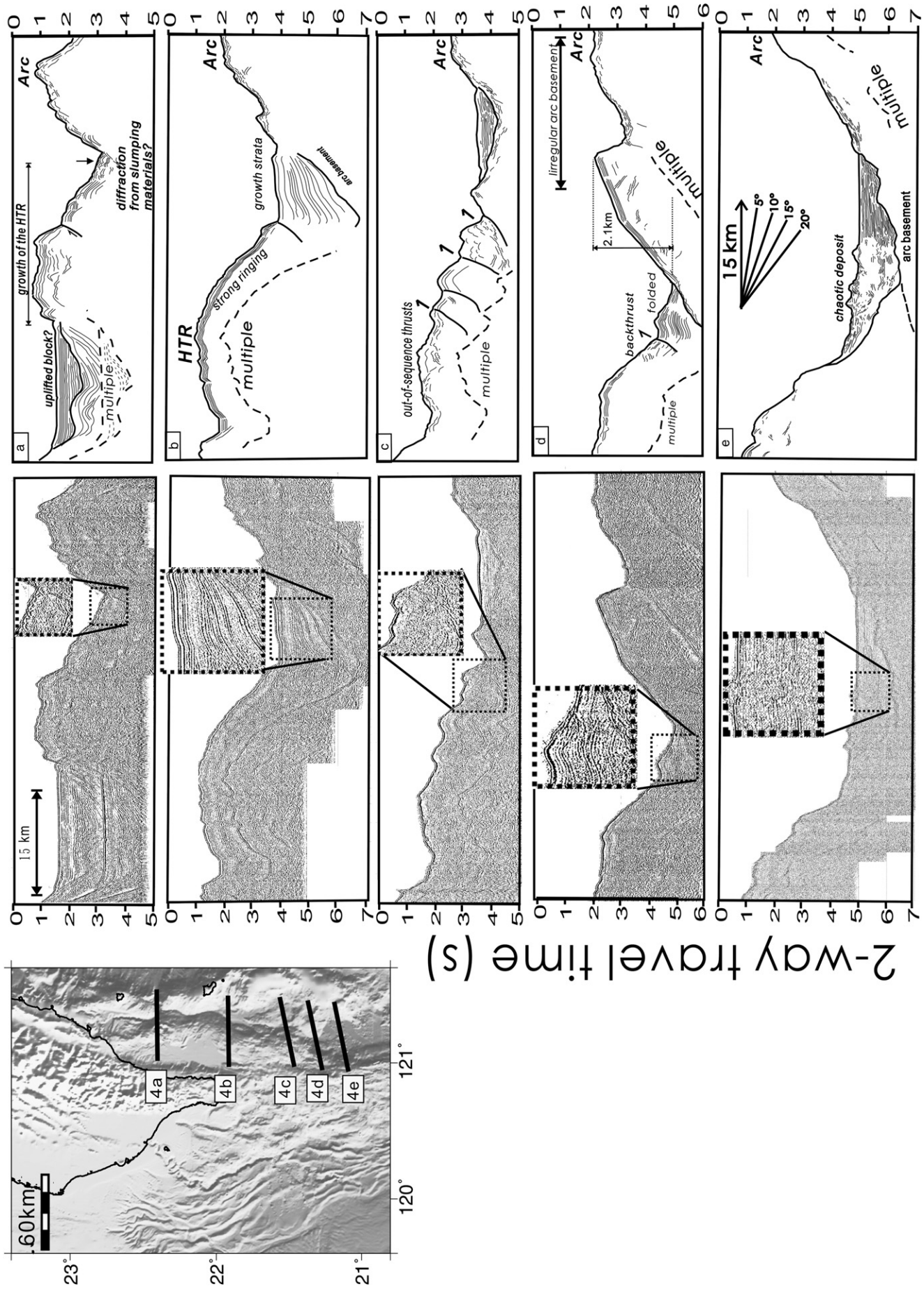

Please cite this article as: Hirtzel, J., et al., Destruction of Luzon forearc basin from subduction to Taiwan arc–continent collision, Tectonophysics (2009), doi:10.1016/j.tecto.2009.01.032

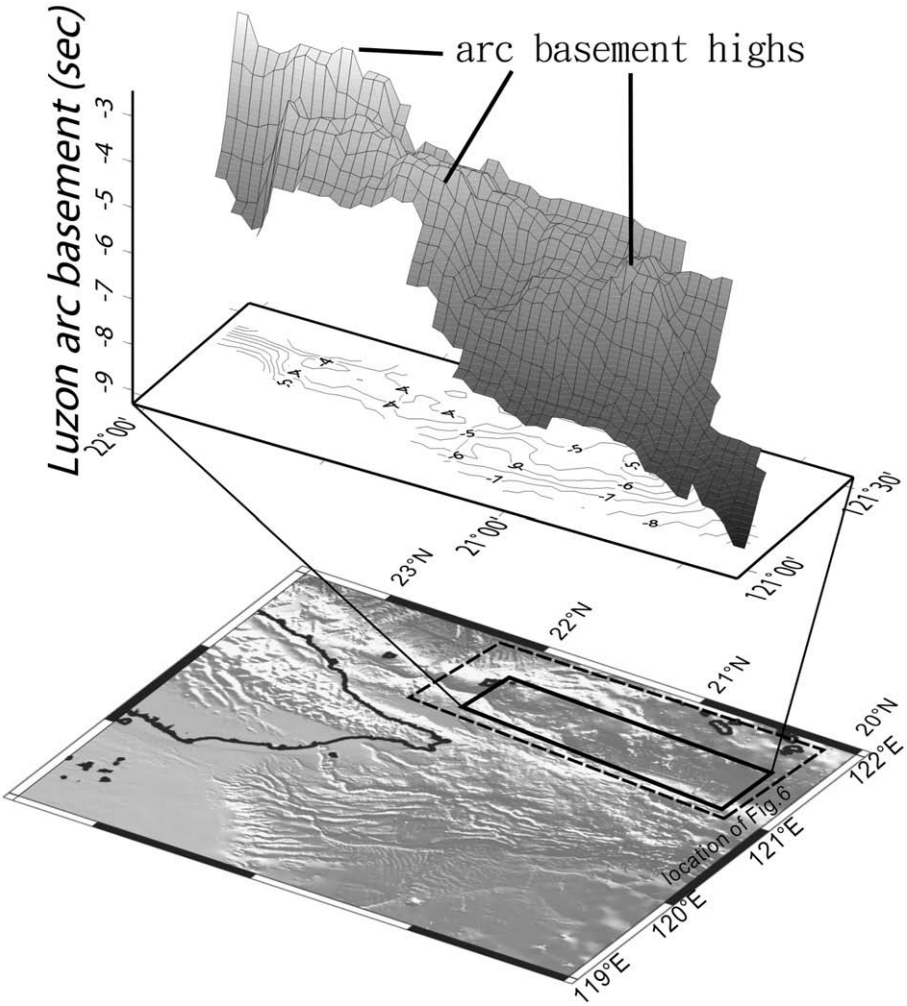

Fig. 5. Two-way traveltime contour map of the volcanic arc basement. This includes the traveltimes of the water column and forearc strata above the basement. Note the very irregular shape of the arc basement slope, which affects the deformation of the forearc basin strata. Note several basement highs have been observed in the initial collision zone and collision zone. The dashed line box marks the location of Fig. 6.

of the accretionary prism. Once incorporated, the sediments are subjected to uplift on the order of 1000 m as the tectonic wedge migrates eastward. Gravity models (Chi et al., 2003) show that the tectonic wedge is mostly sedimentary.

The lack of major unconformities in forearc basin strata in the middle and eastern side of the forearc basin suggests the absence of significant tilting or flexure of the volcanic arc basement. Consequently, thrust loading caused by backthrusting appears to be minor or absent. Small deep-sea fan deposits were found, especially near the volcanic arc and intra-arc basins (e.g. Fig. 3).

5.2. Initial arc–continent collision (between 20°50′N and 21°20′N)

As the continent ocean boundary of the Chinese passive margin enters into the Manila trench, the deformation in the forearc region intensified. Part of the tectonic wedge in this region is composed of exhumed high density materials based on gravity modeling (Chi et al., 2003), suggesting basement involved deformation that brings the high density materials to shallow depths. Next we study the stratigraphic response to these intensified deformations.

The uplifted region on the western side of the basin due to tectonic wedging has produced extensive debris-flow deposits and subject to processes of mass wasting on slopes greater than 15°. As a result, the reflectors on the western side of the forearc basin strata are more chaotic compared with the clean reflectors found on the eastern half of the forearc strata (Fig. 4e). Some of the chaotic strata are also due to the fans with sediments derived from the collision zone to the north.

In the middle and eastern parts of the forearc basin the basement is shallower than that in the subduction zone. The topography of the top of the basement shows large reliefs even though the overlying strata are relatively flat. At latitude near 20°50′N where subduction changes into an initial collision, there is an EW-trending basement high (Fig. 3) where the overlying forearc strata in the initial collision zone become thinner (Fig. 6). In sequences 3 to 6 (especially sequence 3) the strata in the initial collision zone appear to shift slightly to the west. Whether this shift is due to a left-lateral strike-slip fault is still unclear, because the offset is less obvious in the older strata in sequences 7 to 9. And we have not yet found clear flower structures in a N–S seismic line crossing this region (Fig. 7).

Also in sequences 1 and 2, we found small sediment thickness decreases toward a basement bathymetric high at 21°05′N, 121°20′E (Fig. 6). We interpreted this as another evidence of minor but active basement deformation in this region.

Near these rough basement topographies, heat flow estimates give a bit higher (up to 60 °C/km) geothermal gradients (Chi et al., 1998; Chi and Reed, 2008). Several mechanisms can increase the heat flows in these regions, including intrusion of magma bodies, and active fluid migration due to minor faulting or differential compaction of the strata in these regions. Detailed heat flow and hydrological data are needed before we can better understand these abnormal heat flows.

Please cite this article as: Hirtzel, J., et al., Destruction of Luzon forearc basin from subduction to Taiwan arc–continent collision, Tectonophysics (2009), doi:10.1016/j.tecto.2009.01.032

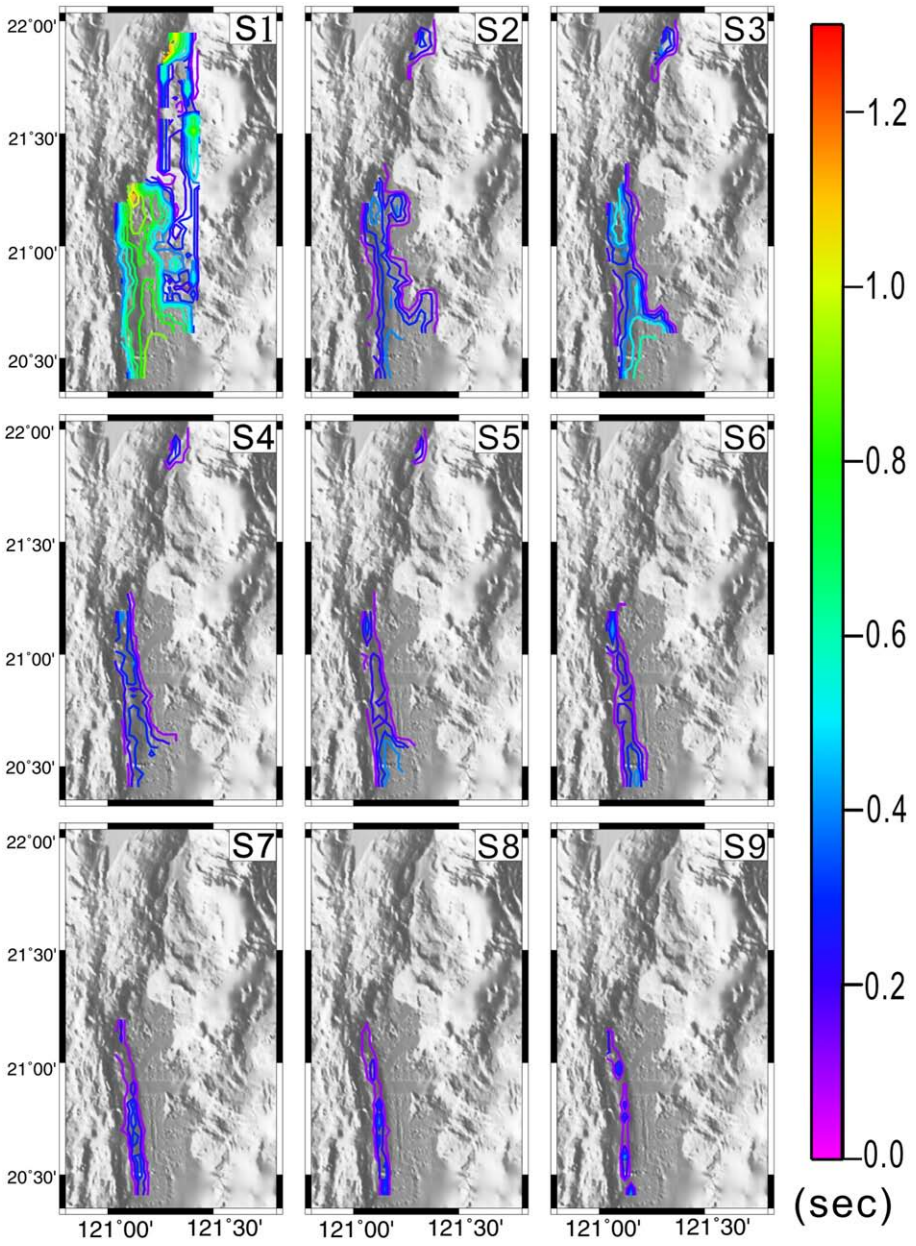

Fig. 6. The isochron maps of the nine sequences derived from this study. See Fig. 5 for location. We used these maps to derive models for deformations of the forearc strata and arc basement. Because the lower sequences cover less areal extents, we have wider spatial controls for the deformation in more recent time. S9 through S4 have depocenter axes along the rear of the accretionary prism with symmetric geometry. On the other hand, sequences 3 through 1 are wedge shapes related to tectonic wedging processes. We also found thicker sediments at the northern end of the closed forearc basin that we interpreted as slump sediments from the north in Huatung Ridge (c.f. S1 and Fig. 4a).

Just south of 21°20′N where the North Luzon Trough closes, we found up to 1.6 s (sequences 1 and 2), relatively flat forearc basin strata lap onto the steep arc basement slope (Fig. 7). This suggests that there is no recent large scale differential uplift of arc basement at the northern part of the North Luzon Trough, even though the basement bathymetry rises over 2200 meters north of this region (Fig. 4d). However, just 20 km to the north, we see growth strata over the inferred deforming arc (Fig. 4c). As a result, this region marks the transition zone separating the different modes of arc basement deformation on both sides, at least while sequences 1 and 2 were deposited and while the arc basement deformation to the north is active. Chemenda et al. (2001) have previously proposed this region as a major boundary separating different deformation styles based on analog modeling and bathymetry data. Chen (2006) has also argued that this is a major boundary in terms of deformation style based on seismic profile interpretation.

5.3. Arc–continent collision (north of 21°20′N)

Further to the north where the major forearc basin is closed and the Huatung Ridge is formed, very active arc deformation has been proposed (Lundberg et al., 1997; McIntosh et al., 2005) based on GPS (Yu et al., 1995), earthquake (Kao et al., 2000), marine geophysical (Malavieille et al., 2002) and multi-channel data (Lundberg et al., 1992; Huang et al., 2006). Here GPS measurements between Taiwan and its neighbor islands show >1.5 cm/yr of shortening. Seismic profiles show active growth strata in the Southern Longitudinal trough, a major successive basin north of the North Luzon Trough. Some of the deformations are episodic, as the growth strata in Fig. 4b show different depositional phases. The shallow part of the profile is hard to interpret due to the strong ringing near the seafloor. Earthquake location and focal mechanisms show active seismicity with mostly strike-slip and reverse faulting in shallow depth and

Please cite this article as: Hirtzel, J., et al., Destruction of Luzon forearc basin from subduction to Taiwan arc–continent collision, Tectonophysics (2009), doi:10.1016/j.tecto.2009.01.032

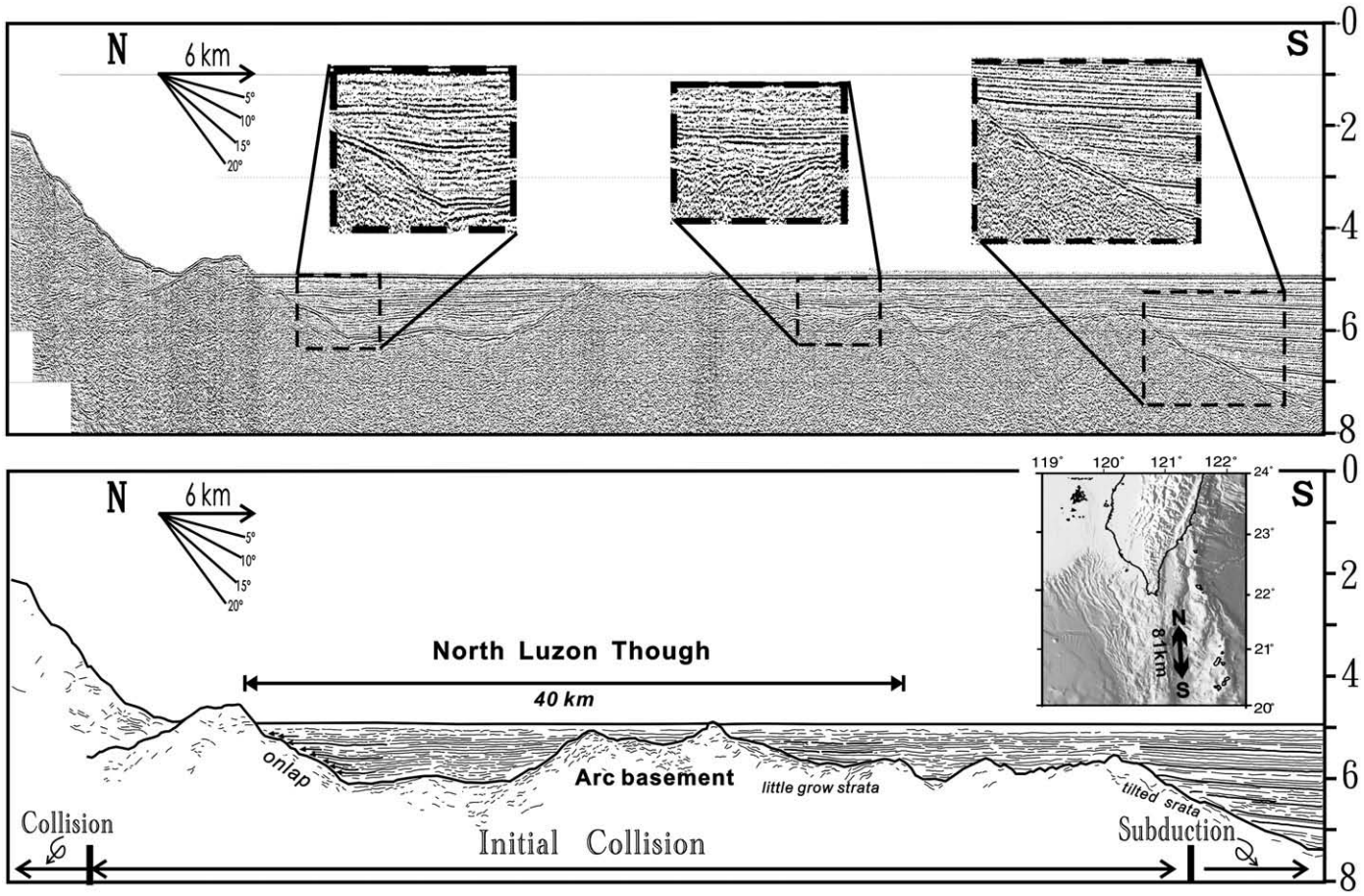

Fig. 7. A N–S line near the northern half of the North Luzon Trough, showing relatively flat reflectors onlapping the forearc basin basement. We inferred that there is no recent large differential tilting of the arc basement in this initial collision zone, based on these overlying flat young strata. The deformation of the arc might be segmented, and there might be an important boundary fault system just north of this region in the collision zone, separating the relatively undeformed arc here and the active arc deformation to the north in the collision zone. The southern end of this profile shows a deeper arc basement in the subduction zone.

forearc basement. There are also arc deformations east of the Huatung ridge, at least at depth, as inferred from seismicity (Kao et al., 2000) and large-offset traveltime inversions (McIntosh et al., 2005).

In response to the shortening in the forearc basement to the north, the east-vergent backthrusts in the subduction zone have propagated further arcward and connect to the east-vergent backthrust underneath the Huatung ridge, consistent with recent sandbox modeling results (Malavieille and Trullenque, 2007). In this sense, the arc basement deformation has helped form the Huatung ridge. However, it was difficult to use the strata to derive detail basement structures because these strata are also influenced by backthrusting, its conjugate faulting, and sediments from the north onland. The rough bathymetry and water multiples it produced also complicated the interpretation.

However, the shallow structures in the successive basins in the region are mostly dipping to the west, opposite to the proposed east-dipping lithospheric fault at depth. An arcward vergent backthrust on top of the deformed arc basement has been proposed to separate these two different domains (McIntosh et al., 2005).

Backthrusting in this region west of the Southern Longitudinal trough exhumes some basement material, based on the general continuity of gravity anomaly here and further to the south in the initial collision zone where detailed gravity modeling has been conducted (Chi et al., 2003). However, it is still not clear if the Southern Longitudinal trough and Huatung ridge are composed mostly of sedimentary materials. If they are mostly sediment, this implies that exhumation alone could not consume the large volume of missing forearc basin basement in this region and subduction of the basement is also at work in this region.

6. Conclusions

Arc basement deformation and tectonic wedging cause the closure of the forearc basin in the collision zone. Using seismic profiles, we have studied the evolution of the Luzon arc and its forearc basin from subduction to collision. Based on seismic stratigraphic analysis of the forearc basin strata, we divided the whole strata into 9 sequences with sequence 1 at the top. The boundary between sequence 3 and sequence 4 is significant for dating the timing of the uplift of forearc basin sediments due to backthrusting along the rear of Taiwan's offshore accretionary prism. This backthrusting, coupled with the arcward migration of a tectonic wedge beneath forearc basin sediments, resulted in multiple cycles of uplift and possible mass wasting of sediments within the North Luzon Trough. On the eastern (arcward) side of the basin, we found relatively undisturbed strata, showing only small amounts of deformation in the subduction zone. Some small deformations have involved forearc basement and helped in generating the irregular basement topography in the initial collision zone. As the collision process continues, the arc basement becomes even shallower in the collision zone where the forearc basin basement has been consumed. Going from south to the north, we also observed abrupt topography changes of the arc basement. Particularly, north of 21°20′N where the North Luzon Trough closes, the basement becomes much shallower with a relief of more than 2200 m, which marks the location of the transition from less deformed arc in the initial collision zone and intensive arc deformation to the north in the collision zone. The majority of this 2200 m relief is not caused by recent active deformation, as we found relatively flat young strata in the North

Please cite this article as: Hirtzel, J., et al., Destruction of Luzon forearc basin from subduction to Taiwan arc–continent collision, Tectonophysics (2009), doi:10.1016/j.tecto.2009.01.032

Luzon Trough lapping onto it. North of this boundary, there are several successive basins and a major bathymetry high called the Huatung Ridge. The stratigraphy, GPS, and earthquake data all show very active shorting in this region.

Acknowledgements

This is an IGCP 524 publication. Parts of the data from this study are based on the MS thesis works of Justin Hirtzel and Liwen Chen. We thank editors Prof. Dennis Brown and Prof. C.Y. Huang. The comments from the editors and two reviewers are helpful. This research was partially supported by the Taiwan Earthquake Research Center (TEC) funded through National Science Council (NSC) with grant number NSC 97-2745-M-001-011 to WCC, and NSF Grant OCE-9416583 to Donald Reed. The TEC contribution number for this article is 00052. This is contribution number IESAS1336 of the Institute of Earth Sciences, Academia Sinica.

References

Bowin, C., Lu, R.-S., Lee, C.-S., Schouten, H., 1978. Plate convergence and accretion in Taiwan–Luzon region. American Association of Petroleum Geologists Bulletin 62 (9), 1645–1672.

Brown, D., Alvarez-Marron, J., Perez-Estaun, A., Puchkov, V., Gorozhanina, Y., Ayarza, P., 2001. Structure and evolution of the Magnitogorsk forearc basin: identifying upper crustal processes during arc–continent collision in the southern Urals. Tectonics 20 (3), 364–375.

Byrne, T., Crepsi, J., 1997. Introduction to the Geology of Taiwan: Field Guidebook for the International Conference and Sino-American Symposium on Tectonic of East Asia, pp. 5–15.

Carena, S., Suppe, J., Kao, H., 2002. Active detachment of Taiwan illuminated by small earthquakes and its control of first-order topography. Geology 30, 935–938.

Chemenda, A.I., Yang, R.-K., Hsieh, C.-H., Groholsky, A.L., 1997. Evolutionary model for the Taiwan collision based on physical modelling. Tectonophysics 274, 253–274.

Chemenda, A.I., Yang, R.-K., Stephan, J.-F., Konstantinovskaya, E.A., Ivanov, G.M., 2001. New results from physical modeling of arc–continent collision in Taiwan: evolutionary model. Tectonophysics 333, 159–178.

Chen, Liwen, 2006. Structural Characteristics and Evolution of the Forearc Basin Offshore Southeastern Taiwan. Master's Thesis, National Taiwan University. 91 pp. (in Chinese).

Chen, A.T., Nakamura, Y., 1998. Velocity structure beneath the eastern offshore region of southern Taiwan based on OBS data. Terrestrial, Atmospheric and Oceanic Sciences (TAO) 9 (3), 409–424.

Cheng, Win-Bin, Wang, Chengsung, Shyu, Chuen-Tien, Shin, Tzay-Chyn, 1998. A three-dimensional Vp model of the southeastern Taiwan area and its tectonic implications. Terrestrial, Atmospheric and Oceanic Sciences (TAO) 9 (3), 425–452.

Chi, Wu-Cheng, Dreger, Doug, 2004. Crustal deformation in Taiwan: results from finite source inversions of six Mw>5.8 Chi–Chi aftershocks. Journal of Geophysical Research 109, B07305. doi:10.1029/2003JB002606.

Chi, Wu-Cheng, Reed, D., 2008. Evolution of shallow, crustal thermal structure from subduction to collision: an example from Taiwan. Geological Society of America Bulletin 120 (5/6), 679–690. doi:10.1130/B26210.1.

Chi, Wu-Cheng, Reed, D., Liu, C.S., Lundberg, N., 1998. Distribution of the bottom-simulating reflector in the offshore Taiwan collision zone. Terrestrial, Atmospheric and Oceanic Sciences (TAO) 9 (4), 779–794.

Chi, Wu-Cheng, Reed, D., Moore, G., Nguyen, T., Liu, C.S., Lundberg, N., 2003. Tectonic wedging along the rear of the offshore Taiwan accretionary prism. Tectonophysics 374, 199–217.

Dorsey, R., 1992. Collapse of the Luzon volcanic arc during onset of arc–continent collision: evidence from a Miocene–Pliocene unconformity, eastern Taiwan. Tectonics 11 (2), 177–191.

Hirtzel, J.O., 1996. Evolution of a Forearc Basin in Arc–Continent Collision, Offshore Taiwan. Master's Thesis, San Jose State University. 41 pp.

Huang, C.Y., Yuan, P.B., Tsao, S.J., 2006. Temporal and spatial records of active arc–continent collision in Taiwan: a synthesis. Geological Society of America Bulletin 118 (3/4), 274–288.

Jahn, Bor-ming, 2004. The Central Asian Orogenic Belt and growth of the continental crust in the Phanerozoic. In: Malpas, J., Fletcher, C.J.N., Aitchison, J.C. (Eds.), Aspects of the Tectonic Evolution of China. Geol. Soc. London. Spec. Pub., vol. 226, pp. 73–100.

Jahn, Bor-ming, Windley, B., Natal'in, B., Dobretsov, N., 2004. Preface—Phanerozoic continental growth in Central Asia. Preface. Journal of Asian Earth Sciences 23, 599–603.

Kao, Honn, Huang, Gqo-Ching, Liu, Char-Shine, 2000. Transition from oblique subduction to collision in the northern Luzon arc–Taiwan region: constraints from bathymetry and seismic observations. Journal of Geophysical Research 105, 3059–3080.

Kim, K.-H., Chiu, J.M., Pujol, J., Chen, K.C., Huang, B.S., Yeh, Y.H., Shen, P., 2005. Three-dimensional V_P and V_S structural models associated with the active subduction and collision tectonics in the Taiwan region. Geophysical Journal International 162 (1), 204–220. doi:10.1111/j.1365-246X.2005.02657.x.

Lee, T.-Q., Kissel, C., Barrier, E., Laj, C., Chi, W.-R., 1991. Paleomagnetic evidence for a diachronic clockwise rotation of the Coastal Range, eastern Taiwan. Earth and Planetary Science Letters 104 (2–4), 245–257.

Liu, Char-Shine, Liu, S.Y., Kao, Ban-Yuan, Lundberg, N., Reed, D.L., 1992. Characteristics of the gravity and magnetic anomalies off southern Taiwan. Acta Geologica Taiwanica 30, 123–130.

Lo, C.H., Onstott, T.C., Chen, C.H., Lee, T., 1994. An assessment of $^{40}Ar/^{39}Ar$ dating for the whole-rock volcanic samples from the Luzon Arc near Taiwan. Chemical Geology. Isotope Geoscience Section 114, 157–178.

Lundberg, N., Reed, D.L., Liu, Char-Shine, Lieske Jr., J., 1992. Structural controls on orogenic sedimentation, submarine Taiwan collision. Acta Geologica Taiwanica 30, 131–140.

Lundberg, N., Reed, D.L., Liu, Char-Shine, Lieske Jr., J., 1997. Forearc-basin closure and arc accretion in the submarine suture zone south of Taiwan. Tectonophysics 274, 5–23.

Malavieille, J., Trullenque, G., 2007. Consequences of continental subduction on forearc basin and accretionary wedge deformation in SE Taiwan: insights from analogue modeling. Tectonophysics. doi:10.1016/j.tecto.2007.11.016.

Malavieille, J., Lallemand, S.E., Dominguez, S., Deschamps, A., Lu, Chia-Yu, Liu, Char-Shine, Schnurle, P., the ACT Scientific Crew, 2002. Arc–continent collision in Taiwan: new marine observations and tectonic evolution. In: Byrne, T.B., Liu, C.-S. (Eds.), Geology and Geophysics of an Arc–Continent collision, Taiwan. Geological Society of America Special Paper, vol. 358, pp. 187–211. Boulder, Colorado.

McCourt, W.J., Aspden, J.A., Brook, M., 1984. New geological and geochronological data from the Colombian Andes: continental growth by multiple accretion. Journal of the Geological Society (London) 141 (5), 831–845. doi:10.1144/gsjgs.141.5.0831.

McIntosh, K., Nakamura, Y., Wang, T.K., Shih, R.C., Chen, A., Liu, C.S., 2005. Crustal-scale seismic profiles across Taiwan and the western Philippine Sea. Tectonophysics 401, 23–54.

Reed, D.L., Lundberg, N., Liu, Char-Shine, Kuo, B.-Y., 1992. Structural relations along the margins of the offshore Taiwan accretionary wedge; implication for accretion and crustal kinematics. Acta Geologica Taiwanica 30, 105–122.

Suppe, J., 1984. Kinematics of arc–continent collision, flipping of subduction, and back-arc spreading near Taiwan. Memoir of the Geological Society of China 6, 21–33.

Tang, J.-C., Chemenda, A.I., 2000. Numerical modeling of arc–continent collision: application to Taiwan. Tectonophysics 325, 23–42.

Teng, L.S., 1990. Tectonic evolution of late Cenozoic arc–continent collision in Taiwan. American Association of Petroleum Bulletin 74 (6), 1004–1005.

Yang, T.F., Chen, C.-H., Tien, R.L., Song, S.R., Liu, T.K., 2003. Remnant magmatic activity in the Coastal Range of East Taiwan after arc–continent collision: fission-track data and $^{3}He/^{4}He$ ratio evidence. Radiation Measurements 36, 343–349.

Yu, Shui-Beih, Chen, Horng-Yue, Kuo, Long-Chen, 1995. Velocity field of GPS stations in the Taiwan area. Tectonophysics 274, 41–59.

Please cite this article as: Hirtzel, J., et al., Destruction of Luzon forearc basin from subduction to Taiwan arc–continent collision, Tectonophysics (2009), doi:10.1016/j.tecto.2009.01.032